

Research on Neuro-Adaptive Fault-Tolerant Control method for Large Floating Wind Turbine

Lei Wang¹, Fangjun Jin¹, Yang Gao^{2,3}, Xin Du², Zhihong Zhang², Zhiliang Xu², Jiongming Yang²

1 College of Automation, Chongqing University, Chongqing, 400044, PR China

2 Xinjiang Goldwind Science And Technology Co., Ltd.

3 College of Architecture Engineering, Tianjin University, Tianjin, 300072, PR China

ABSTRACT

The pitch system plays a key role in the large offshore wind turbine for regulating pitch angle to the desired one and hence to stabilize the power out. However, due to the uncertainty of time-varying parameters and various unknown disturbances acting on the turbine blades, accurate and rapid regulation of pitch angle can hardly be achieved using the existing available pitch control strategy. Moreover, the actuator faults of the pitch system may occur in the long-term operation of the wind turbine, which greatly reduces the reliability and power generation efficiency. Aiming at the above problems, a nonlinear model of the pitch system considering time-varying parameter uncertainties and unknown disturbances is established, based on which a neural adaptive fault-tolerant control strategy with a rate function is proposed. A co-simulation is developed, and the merits of the proposed method are verified.

Keywords: Floating wind turbine, Pitch system, Fault-tolerant control, Pitch angle tracking.

NONMENCLATURE

Abbreviations

CPC	Collective Pitch Control
IPC	Individual Pitch Control
FDD	Fault Detection and Diagnosis
FTC	Fault-Tolerant Control
RBFNN	Radial Basis Function Neural Network

1. INTRODUCTION

Offshore wind turbines (WTs) are developing these days rapidly, and floating WT technology has been seen as an effective solution to the energy crisis and environmental pollution [1]. For an offshore floating WT, it is typically required stable power output and load mitigation to increase service life and lower maintenance costs [2]. Generally, this objective can be achieved via pitch control mechanisms.

Current designs employ collective pitch control (CPC) and individual pitch control (IPC) techniques, in which the IPC has been deemed a more effective way for mitigating the load without affecting the turbine's power output [3]. In [4], a fuzzy logic IPC is proposed to address parameter uncertainties and random disturbances for a WT pitch system, which highly depends on predefined fuzzy rules. Besides, other strategies such as PID control, model predictive control, and robust adaptive control under an IPC scheme were developed in previous studies to achieve stable power output and improve the robustness of the closed-loop system.

The methods reported in above studies consider ideal sensing and actuation, assuming that the sensor is reliable and the contribution due to changes in actuator dynamics is negligible. However, the actuators of the pitch system are prone to faults during the operation of the wind turbine in the presence of highly varying stochastic loads [5]. Fault detection and diagnosis (FDD) and fault-tolerant control (FTC) provide an effective way to against sensor and actuator faults in wind turbines [6]. FDD/FTC schemes for wind turbine's pitch system have been significantly studied over the years (for example, see [7]). However, only a few studies involving the combination of IPC in wind turbines and FDD/FTC in the presence of faults are reported. In addition, only a very specific and less severe type of fault was considered.

Typically, most FTC methods are based on a FDD process for fault identification, which usually involves complex analyses and numerical calculations. Furthermore, far too little attention has been paid to the nonlinear dynamic characteristic of the system in aforementioned studies, which treat the pitch actuator as a linear second-order system or be linearizable. Also, the error of modeling nonlinear pitch systems caused by the external disturbances and parameter varying are generally not taken into account in the design of the FTC, which makes it difficult to distinguish between faults and modeling uncertainties in practical applications. Neural networks based control scheme can make full use of the observation data, learn and modify parameters online, which is deemed promising in handling system uncertainties and disturbances [8]. In addition, the currently available FTC methods are commonly useful for

Selection and peer-review under responsibility of the scientific committee of the 13th Int. Conf. on Applied Energy (ICAE2021).

Copyright © 2021 ICAE

a slow time-varying system, while the pitch angle needs to regulate a desired one in some specific situations.

Motivated by these questions and comparing with the above-mentioned literature, this study proposes a fault-tolerant control strategy based radial basis function neural network (RBFNN), aiming to provide a solution to the difficulty of quick and accurate pitch regulation for large offshore floating WT's pitch system under actuation failures. The paper is organized as follows. Section 2 establishes the nonlinear dynamic model of the pitch system. In Section 3, the fault-tolerant pitch tracking controller is proposed. In Section 4, co-simulation on a 5MW floating wind turbine model is developed to verify the validity of the proposed control strategy. Finally, conclusions are made in Section 5.

2. MODELING OF THE PITCH SYSTEM AND PROBLEM FORMULATION

2.1 Pitch system model

The National Renewable Energy Laboratory (NREL) 5MW floating wind turbine model was employed in this study; As shown in Fig. 1 which depict the blade pitch adjustment mechanism, there exists a highly nonlinear relationship between the driving force and the pitch angle during the pitch angle adjustment process.

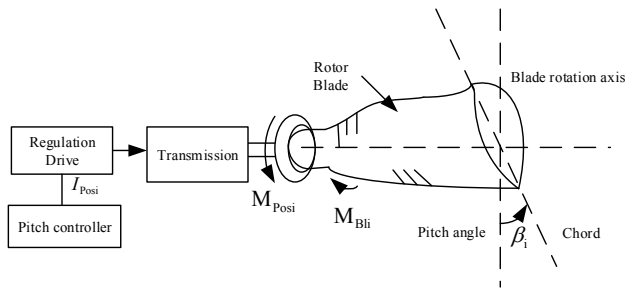


Fig. 1. The schematic diagram describing the blade pitch adjustment mechanism.

From Fig. 1, the differential equation describing the aerodynamic dynamics characteristics of the pitch system can be easily obtained.

$$\begin{aligned} & (J_{LBi} + J_{BLi}) \ddot{\beta}_i + \left(\frac{dJ_{LBi}}{dt} + \frac{dJ_{BLi}}{dt} + k_{DBi} + k_{RLi} \right) \dot{\beta}_i \\ & + \left(\frac{dk_{DBi}}{dt} + \frac{dk_{RLi}}{dt} \right) \beta_i = M_{Posi} - M_{Bli} \end{aligned} \quad (1)$$

$$\begin{aligned} M_{Bli} = & M_{Pri} + M_{Lifi} + M_{Ti} + M_{Bendi} + M_{Teeteri} \\ & + M_{Fricti} + \delta_i(\beta_1, \beta_2, \beta_3) \end{aligned} \quad (2)$$

$$M_{Posi} = C_{Ti} I_{Posi} \quad (3)$$

where J_{LBi} and J_{BLi} denote the inertia coefficient of the accelerated air and the mass moment of inertia of the unit blade along its longitudinal axis, respectively; k_{DBi} and k_{RLi}

represents the damping coefficient and the friction coefficient of the bearing respectively; M_{Posi} and M_{Fricti} are the driven torque and friction torque, respectively; M_{Lifi} , M_{Bendi} and $M_{Teeteri}$ are the lifting moment, bending moment and the tilting moment; I_{Posi} denotes the driving current of the servo motor, and C_{Ti} represents the conversion factor between I_{Posi} and M_{Posi} . In this study, M_{Posi} is treated as the control input of the pitch actuator. Additionally, $\delta_i(\beta_1, \beta_2, \beta_3)$ describes the unbalanced loads on the rotor blade, including aerodynamic loads caused by the wind shear effect, tower shadow effect, and turbulence-induced random disturbances, etc.

The dynamic equation describing the pitch adjustment process for three rotor blade given in Eq. (1), exposed with the disturbance can be further expressed as:

$$\mathbf{M}(\cdot) \ddot{\boldsymbol{\beta}} + \mathbf{D}(\cdot) \dot{\boldsymbol{\beta}} + \mathbf{N}(\cdot) \boldsymbol{\beta} + \mathbf{d}(\cdot) = \mathbf{u}_a \quad (4)$$

where $\boldsymbol{\beta} = [\beta_1, \beta_2, \beta_3]^T \in \mathbb{R}^3$ and $\dot{\boldsymbol{\beta}} = [\dot{\beta}_1, \dot{\beta}_2, \dot{\beta}_3]^T \in \mathbb{R}^3$ represent the blade pitch angle and corresponding angular velocity respectively; $\mathbf{N}(\cdot) = \text{diag}(N_1, N_2, N_3) \in \mathbb{R}^{3 \times 3}$,

$$N_i = \left(\frac{dJ_{LBi}}{dt} + \frac{dJ_{BLi}}{dt} + k_{DBi} + k_{RLi} \right), \mathbf{M}(\cdot) = \text{diag}(M_1, M_2, M_3) \in \mathbb{R}^{3 \times 3},$$

$\mathbf{M}_i = J_{LBi} + J_{BLi} > 0$, $\mathbf{d}(\cdot) = \text{diag}(d_1, d_2, d_3) \in \mathbb{R}^{3 \times 3}$ denotes the external disturbance on the pitch system considered to be bounded by $\|d\| < \bar{d}$ where \bar{d} is an unknown finite number which can represent any un-modelled that may affect the system.

$\mathbf{u}_a = [u_{a1}, u_{a2}, u_{a3}]^T \in \mathbb{R}^3$ is the control input.

The problem formulation as: Considering the given smooth desired trajectory pitch angle $\boldsymbol{\beta}^* = [\beta_1^*, \beta_2^*, \beta_3^*]^T$, for the pitch system dynamics given by Eq.(4), find the pitch actuator input torques \mathbf{u}_a such that the pitch system states $\boldsymbol{\beta} = [\beta_1, \beta_2, \beta_3]^T$ track a given desired pitch angle $\boldsymbol{\beta}^*$ as closely and fast as possible.

2.2 Faults in pitch actuator

It should be noted that in the long-term operation of WT, unforeseen failures may occur in the pitch system. Actuators partially lose effectiveness are considered in this work, and the failure model is shown in Fig. 2. Generally, the relationship between \mathbf{u} and \mathbf{u}_a can be expressed as:

$$\mathbf{u}_a = \boldsymbol{\rho}(t) \mathbf{u} + \mathbf{u}_r \quad (5)$$

where $\boldsymbol{\rho}(t) = \text{diag}\{\rho_1(t), \rho_2(t), \rho_3(t)\}$ is a diagonal matrix; the element $\rho_i(t) \in (0, 1], (i = 1, 2, 3)$ is a time-varying scalar function called the ‘‘health factor’’ for i th pitch actuator, indicating the actuation effectiveness; $\mathbf{u}_r = [u_{r1}, u_{r2}, u_{r3}]^T$ is an unknown vector function, which reflects the uncontrollable part of the actuator when it fails.

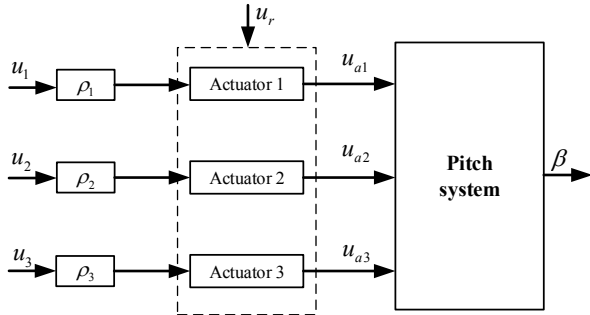


Fig. 2. Blade Pitch Control system under actuation failure.

2.3 Preliminaries

Based on the known approximation property, given a smooth continuous nonlinear scalar function $L(x)$ in a compact set Ω_x , there exists an ideal RBFNN that can approximate $L(x)$ to arbitrary precision with the form

$$L(x) = \mathbf{W}^T \mathbf{S}(x) + \epsilon(x), |\epsilon(x)| \leq \bar{\epsilon}, \forall x \in \Omega_x \quad (6)$$

where $\mathbf{W} \in \mathbb{R}^p$ is a weight vector with p nodes, $\mathbf{S}(x) = [S_1(x), \dots, S_p(x)]^T \in \mathbb{R}^p$ is a basic function vector, $\epsilon(x)$ is an approximation error, and $\bar{\epsilon}$ is a constant. $S_i(x)$ was chosen as a Gaussian function in this study, which is derived as

$$S_i(x) = \exp\left(-\frac{(x - \tau_i)^T (x - \tau_i)}{2\psi^2}\right) \quad (7)$$

where $\tau_i (i=1, \dots, p)$ and ψ are constants, representing the center and width of the base function respectively.

Motivated by [9], a time-varying speed function $\vartheta(t)$ is introduced,

$$\vartheta(t) = \frac{1}{(1 - b_f)\kappa(t)^{-1} + b_f} \quad (8)$$

where $0 < b_f < 1$ is a free parameter chosen by the designer. $\kappa(t)$ is a function selecting from the rate function pool, which is defined as:

$$\kappa(t) = \begin{cases} \left(\frac{T_0}{T_0 - t}\right)^4 \bar{\kappa}(t) & 0 \leq t < T_0 \\ \infty & t \geq T_0 \end{cases} \quad (9)$$

where $0 < T_0 < \infty$ is a given finite time. $\bar{\kappa}(t)$ is a smooth monotonically increasing function, satisfying $\bar{\kappa}(0) = 1$ and $\dot{\kappa} \geq 0$, and many functions such as $1, 1+t^2, e^t, 2e^t-1$ can be selected. It follows that $\lim_{t \rightarrow T_0} \left(\frac{T_0}{T_0 - t}\right)^4 \bar{\kappa}(t) = \infty$ to ensure $\kappa(t)$ is continuous. $\vartheta(t)$ is adjustable by choosing different T_0 and b_f . This study only focuses on the effects of b_f on $\vartheta(t)$, which affects the tracking speed.

3. CONTROLLER DESIGN

To facilitate the controller design, a pitch angle tracking error vector is introduced as

$$\mathbf{e} = \beta - \beta^* \quad (10)$$

where $\beta = [\beta_1, \beta_2, \beta_3]^T$, $\beta^* = [\beta_1^*, \beta_2^*, \beta_3^*]^T$. Taking the time derivative of (10), the basic error dynamic equation of the closed-loop system was derived as:

$$\begin{aligned} \dot{\mathbf{e}} &= \dot{\beta} - \dot{\beta}^* \\ \ddot{\mathbf{e}} &= \mathbf{M}^{-1}(\rho \mathbf{u} + \mathbf{u}_r - \mathbf{F} - \mathbf{d}) \end{aligned} \quad (11)$$

where $\mathbf{F} = \mathbf{D}\dot{\beta} + \mathbf{N}\beta$ contains all the nonlinearity affecting the system,

Based on this, an error transformation is introduced to improve the tracking performance.

$$\boldsymbol{\varepsilon}(t) = \mathcal{G}(t)\mathbf{e}(t) \quad (12)$$

For later technical design, the following filtered variable [40] is introduced.

$$\mathbf{E}(t) = \lambda \boldsymbol{\varepsilon}(t) + \dot{\boldsymbol{\varepsilon}}(t) \quad (13)$$

where $\lambda > 0$ is a user-defined parameter. It can be concluded that if $\lim_{t \rightarrow \infty} E_i = 0$, then $\lim_{t \rightarrow \infty} \boldsymbol{\varepsilon}_i = 0$ and $\lim_{t \rightarrow \infty} \dot{\boldsymbol{\varepsilon}}_i = 0$, sharing the same decreasing rate as that of $E_i(t)$. In addition, the boundedness of $\mathbf{E}(t)$ ensuring the boundedness of $\boldsymbol{\varepsilon}(t)$ and $\dot{\boldsymbol{\varepsilon}}(t)$.

By integration of the rate function $\mathcal{G}(t)$ defined in (9), the accelerated neural adaptive controller is designed as follows:

$$\mathbf{u} = -(\delta \hat{a} \phi^2(x) \varphi^2) \mathcal{G} \mathbf{E} \quad (14)$$

With an updated law of \hat{a} expressed as:

$$\dot{\hat{a}} = -\mu \hat{a} + \delta \mathcal{G}^2 \phi^2(x) \varphi^2 \|\mathbf{E}\|^2 \quad (15)$$

where $\varphi = 1 + \|\boldsymbol{\eta}\| + \frac{1}{2} \|\mathcal{G}^{-1} \mathbf{E}\|$, $\boldsymbol{\eta} = \mathcal{G}^{-1} \mathbf{v}(t) + c_1 \mathcal{G}^{-1} \mathbf{E}(t) - \dot{\beta}^*$,

$\delta > 0, c_1 > 0$ and $\mu > 0$ are user-defined parameters. The radial basis function neural network (RBFNN) is used in this work to approximate the unknown function $\phi(x) = \|\mathbf{S}(x)\| + 1$ with $S_i(x)$ being defined in (7). The block diagram of the proposed RBF neural networks based fault-tolerant control scheme is shown in Fig. 3.

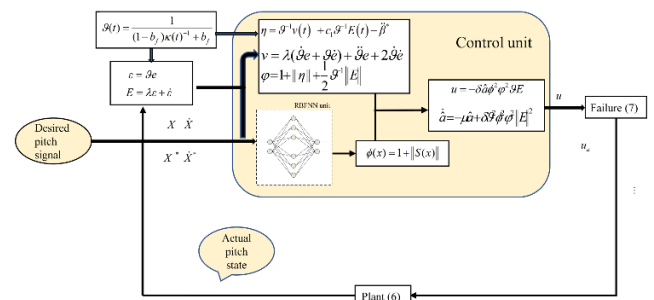


Fig. 3. The block diagram of the proposed neuro-adaptive fault-tolerant control scheme for the floating WT pitch system.

4. SIMULATION RESULTS AND DISCUSSION

In this section, numerical simulations are carried out on a 5MW Spar type wind turbine model developed by FAST and Matlab/Simulink to verify the effectiveness of the proposed

fault-tolerant control strategy. The components of the nonlinear pitch system describing the dynamic characteristics are given as follows:

$$\begin{aligned} M(\cdot) &= \text{diag}(\sin(0.5\beta_1 t) + 2, \sin(0.5\beta_2 t) + 2, \\ &\quad \sin(0.5\beta_3 t) + 2) \\ D(\cdot) &= \text{diag}(\cos(0.5\dot{\beta}_1 + \dot{\beta}_1) + 2, \cos(0.5\dot{\beta}_2 + \dot{\beta}_2) + 2, \\ &\quad \cos(0.5\dot{\beta}_3 + \dot{\beta}_3) + 2) \\ N(\cdot) &= \text{diag}(\cos(0.5\beta_1 + \dot{\beta}_1) / 3 + 1, \cos(0.5\beta_2 + \dot{\beta}_2) / 3 + 1, \\ &\quad \cos(0.5\beta_3 + \dot{\beta}_3) / 3 + 1) \\ d(\cdot) &= [0.5\cos(0.5\beta_1 t) + 3\sin(0.5\dot{\beta}_1) + \sin(0.05t); \\ &\quad 0.5\cos(0.5\beta_2 t) + 3\sin(0.5\dot{\beta}_2) + \sin(0.05(t + 2\pi / 3)); \\ &\quad 0.5\cos(0.5\beta_3 t) + 3\sin(0.5\dot{\beta}_3) + \sin(0.05(t + 4\pi / 3));] \end{aligned} \quad (16)$$

Two different cases are considered in this section to demonstrate the effectiveness of the proposed method. Though the pitch regulation process is individual for each blade, for the sake of brevity, the tracking performance of the pitch angle of rotor blade 1 is only depicted in the following analysis.

Case 1: Tracking normal sinusoidal signal compared to the PI-like sliding mode controller.

In this case, a normal sinusoidal signal is introduced to verify that the RBFNN based control method can achieve a better transient performance compared to the PI like sliding mode control strategy. The desired pitch angle is selected as $\beta^* = 2 + \sin(t)$, and the proposed scheme shares the same system parameters and initial conditions ($\beta = 3^\circ$) with the PI controller. In addition, a white noise signal with a signal-to-noise ratio of 7.13 was introduced in the simulation to verify the capability to cope with unknown disturbances of two different control schemes. To obtain a desired performance, the design variables δ and b_f are chosen as 11 and 0.04, respectively.

The pitch angle tracking process is shown in Fig. 4. Fig. 4 (a) depict the tracking process of the proposed method; it is observed that the two curves, i.e., the desired pitch angle β^* and the actual pitch angle β , are very consistent with each other within a short period of time, which indicates that the proposed controller can achieve a quickly tracking process. Fig. 4 (b) and (c) compare the control variable u_1 tracking error e_1 under PI-like sliding mode controller and proposed controller respectively. It is seen from Fig. 4 (c) that it takes a longer time for the system with PI controller to ensure the tracking error converges to a compact set, which implies that the proposed controller can achieve a better tracking performance. Fig. 4 (b) depicts the control input of two strategies from which one can conclude that the control output of the proposed controller is smoother than that of the PI controller. In addition, the proposed controller can achieve a smoother steady performance, which makes the proposed controller more superior to cope with the unknown disturbance, thus enhance stability and the robustness of the system.

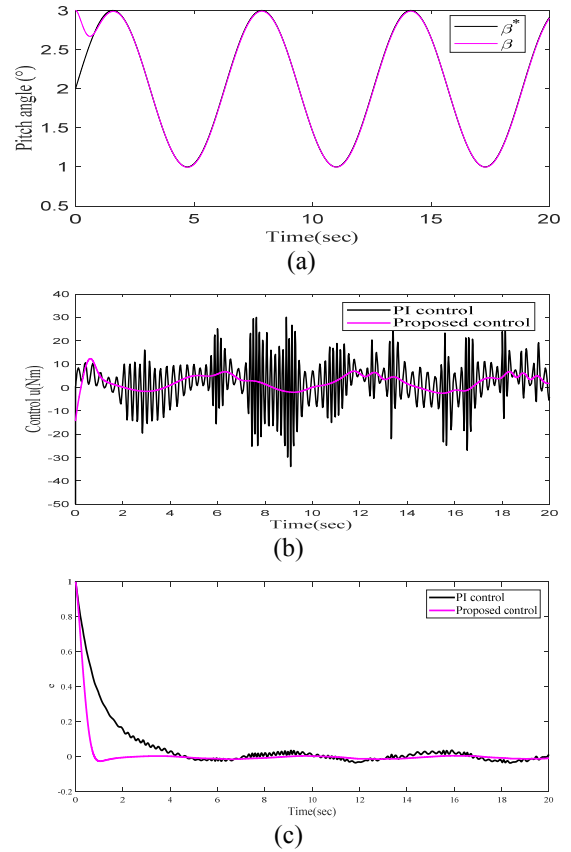


Fig. 4. Simulation diagram.

Case 2 : Fault-tolerance performance.

To ensure that the real pitch angles can track the desired pitch angle under time-varying system parameter, unknown disturbances, and faulty conditions, a faulty actuator case combined with a white noise signal during the operation is considered. The working conditions are depicted in Fig. 5, wherein the WT operating under the wind speed profile 18m/s. Suppose that under a certain situation, the considered WT is operating with a wind profile shown in Fig. 5 (a), wherein the effective wind speed is 18m/s. Three desired pitch angles are as shown in Fig. 5 (b).

In this case, the “healthy factor” of blade pitch 1 ρ_1 suddenly drop to 0.85 at $t=30s$ and became to $\rho_1 = 0.85 - 0.1 * \cos(t)$ at $t = 60s$. The relative controller parameters are the same as the previous cases. The tracking error curve of blade 1 is as shown in Fig. 6. It can be concluded that the proposed controller exhibits excellent robustness to cope with the system uncertainties. The blade pitch tracking error ensures to converge within a small range both on normal condition and faulty actuation case under such control strategy. The generator torque and power output are depicted in Fig. 7. It is noted the value of generator torque maintains a constant as the WT operating above the rated wind speed. To sum up, the proposed neural adaptive fault-tolerant control strategy can achieve desirable transient tracking performance and thus stabilize the power output when the wind turbine is operating under complex environmental load and actuator failure.

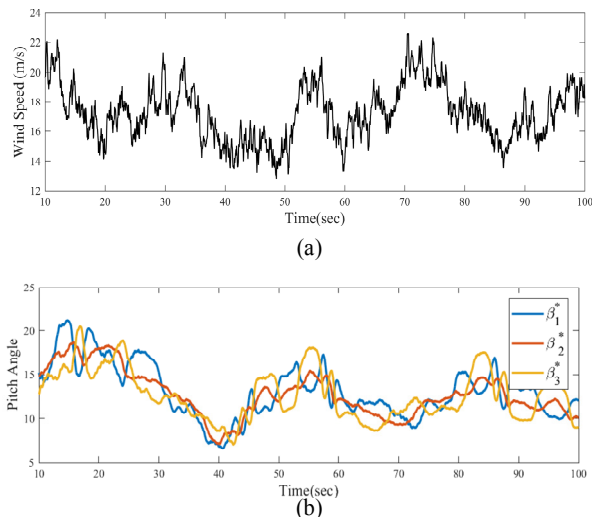


Fig. 5. Simulation diagram of the 18m/s effective wind profile and three desired angles.

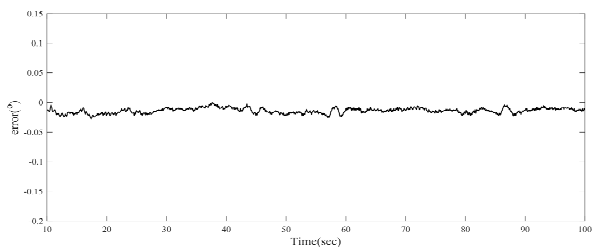


Fig. 6. Tracking error of blade 1 under actuator failure.

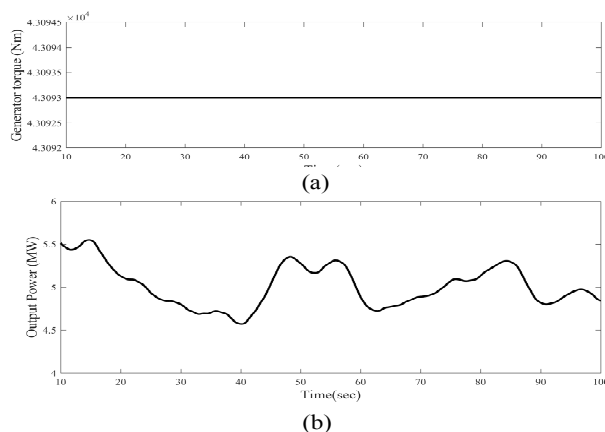


Fig. 7. Generator torque and power output and of the wind turbine system.

5. CONCLUSION

This work studies the problem of fault-tolerant control design for a nonlinear wind turbine pitch system under actuation failure, system parameter uncertainties, and various unknown disturbances. With the proposed control method, the pitch system can quickly and accurately regulate pitch angle to the desired one, thus achieving a stable power output. Besides, the design procedure of the controller does not depend on specific

parameter information about the nonlinear pitch system and actuation faults. Moreover, the utilization of the rate function ensures a transient performance guaranteed tracking during the adjustment process of the pitch angle. The proposed fault-tolerant control method is deemed favorable for high precision tracking performance in the application under various unknown loads and actuator faults.

ACKNOWLEDGEMENT

This work was supported by National Natural Science Foundation of China (No.51875058), the project of Science and technology assistance to Xinjiang (No. 2021E02039).

REFERENCE

- [1] Lee, Joyce, et al: 'Global wind report 2019', Global Wind Energy Council (GWEC), Global Wind Energy Council (GWEC), Brussels, 2020.
- [2] Tiwari, R., Babu, N.R.: 'Recent developments of control strategies for wind energy conversion system', *Renewable and Sustainable Energy Reviews*, 2016, **66**, pp. 268-285.
- [3] Mohammadi, E., Fadaeinedjad, R., Moschopoulos, G.: 'Implementation of internal model based control and individual pitch control to reduce fatigue loads and tower vibrations in wind turbines', *Journal of Sound and Vibration*, 2018, **421**, pp. 132-152.
- [4] Han, B., Zhou, L., Yang, F., Xiang, Z.: 'Individual pitch controller based on fuzzy logic control for wind turbine load mitigation', *IET Renewable Power Generation*, 2016, **10**, (5), pp. 687-693.
- [5] Pandit, R.K., David I.: 'SCADA-based wind turbine anomaly detection using Gaussian process models for wind turbine condition monitoring purposes', *IET Renewable Power Generation*, 2018, **12**, (11), pp. 1249-1255.
- [6] Habibi, H., Howard, I., Simani, S.: 'Reliability improvement of wind turbine power generation using model-based fault detection and fault tolerant control: A review', *Renewable energy*, 2019, **135**, pp. 877-896.
- [7] Cho, S., Zhen, G., Torgeir, M.: 'Model-based fault detection, fault isolation and fault-tolerant control of a blade pitch system in floating wind turbines', *Renewable Energy*, 2018, **120**, pp. 306-321.
- [8] Habibi, H., Rahimi Nohooji, H., Howard, I.: 'Power maximization of variable-speed variable-pitch wind turbines using passive adaptive neural fault-tolerant control', *Frontiers of Mechanical Engineering*, 2017, **12**, pp. 377-388.
- [9] Zhao, K., Song, Y., Ma, T., He, L.: 'Prescribed performance control of uncertain euler-lagrange systems subject to full-state constraints', *IEEE transactions on neural networks and learning systems*, 2017, **29**, (8), pp. 3478-3489.